

Analysis of bone architecture in rodents using micro Computed Tomography

Robert J. van 't Hof PhD, Enrico Dall'Ara PhD

Abstract

This chapter describes the use of micro computed tomography scanning for analysing bone structure, focussing on rodent bone. It discusses sample preparation, the correct setup of the scanner, the impact of some of the important scanner settings and new applications.

Keywords: x-ray, 3D, rodent, computerised tomography, imaging CT, microCT

1. Introduction

Radiological techniques such as plain X-ray and Dual Energy X-ray absorptiometry (DXA) are widely used for the investigation of patients with bone disease in routine clinical practice and similar techniques can be used to examine the skeleton in animal models of bone disease. For example, the Piximus DXA scanner (GE healthcare) has been used to measure bone density in mice and rats and follow the changes in bone density that result from ovariectomy. Similarly radiological analysis of the skeleton in mice and rats can be undertaken using the Faxitron instrument. Although plain X-rays are adequate to detect gross morphological changes in the skeleton of rodents they do not have sufficient resolution to detect subtle changes in bone structure or bone density. Similarly DXA analysis has low sensitivity for detecting the changes in bone density that occur after ovariectomy especially in mice. This is because most of the changes occur in the trabecular bone and DXA scanners cannot separate trabecular from cortical bone. For example, we have found that the Piximus scanner shows bone loss at the proximal tibia of about 5-10% 3-weeks after ovariectomy in mice (which is barely statistically significant using 10 animals per group), while analysis of a similar experiment using μ CT analysis showed a highly significant 30-40% decrease of trabecular bone at the same site.

The current generation of μ CT scanners are the current method of choice for skeletal phenotyping of rodent models of bone disease. In contrast to histomorphometry, μ CT is non-destructive technique, and specialised instruments for μ CT imaging of live animals are now available, which allow the researcher to conduct serial studies during skeletal growth and ageing in mice and rats. Moreover, during the last decade Synchrotron light based μ CT imaging and desktop high-resolution μ CT scanners have been developed to visualize features in bone such as osteocyte

lacunae and canaliculi, which were not visible with other 3D non-destructive imaging techniques, and are now of increasing interest to study peri-lacunar remodelling.

1.1. Micro CT analysis

Micro CT involves taking a series of X-ray images of the sample at different rotations, and then using computer algorithms to reconstruct a 3D image stack (1,2). The process of μ CT analysis can therefore be divided into three different stages.

- 1) Acquiring the X-ray projection images,
- 2) Computerised reconstruction of the 3D stack of images from the projection images
- 3) Analysis of the 3D image stack.

1.2 Acquiring the X-ray projection images

Two different strategies are used to obtain images at different rotations. In most standard desktop μ CT systems, the sample stage containing the specimen to be analysed is rotated, whereas the *in vivo* systems use a gantry to rotate the X-ray source and camera around the sample stage containing the specimen, which is fixed in stationary position. *In vivo* systems tend to be less flexible in the range of resolutions, as the source and camera are in a fixed position relative to one another. The *in vivo* systems also tend to have a lower maximum resolution due to potential effect of movement artefacts. Furthermore, to avoid side effects from prolonged anaesthesia and high ionising radiation doses, scans times need to be kept relatively short, and this may impact scan quality. For these reasons, *in vivo* μ CT systems have a best resolution of 9-10 μ m (although the latest systems claim resolutions around 5-6 μ m),

whereas the desktop systems normally have a best resolution in the 2-5 μm range and systems with $<1\mu\text{m}$ resolution are available.

1.3. Image reconstruction

Most reconstruction software packages use the same Feldkamp cone-beam reconstruction algorithm (3), although faster algorithms have recently been developed. This algorithm is based on filtered-back projection, but it is beyond the scope of this chapter for its details to be discussed here. An important requirement for valid reconstruction is that the X-ray beam is not fully absorbed at any point in the sample; there should always be some transmission at each pixel of the X-ray camera.

1.4 Analysis of the 3D image stack

Many different software packages are available for quantitative analysis of the resulting 3D image stack. Many standard image analysis packages are available that could theoretically handle 3D image stacks, but most users employ specialist software packages that are provided by the manufacturers of μCT systems. The most widely used μCT machines are those manufactured by Scanco and Bruker (former Skyscan) and these instruments have similar capabilities. In this chapter examples of the Skyscan CTAn software are reported for *ex vivo* analyses, while examples of the Scanco Analyses software are reported for *in vivo* applications.

2. Materials

2.1 μCT Scanner

The most commonly used μCT systems for the study of bone disease are manufactured by Scanco and Bruker (former Skyscan). Other systems are also

available however manufactured by GE Healthcare, MILabs and Perkin Elmer. The Skyscan 1172 (or 1272) and Scanco μ CT35 (or 40) are generally used for scanning specimens *ex vivo*, whereas live animals can be scanned *in vivo* using the Skyscan 1076 or the Scanco vivaCT 40 (or 80) systems. Zeiss (former XRadia) provides a new generation scanner that copies the hardware available for Synchrotron facilities and provides sub-micron desktop scanners (e.g. Versa and Ultra systems).

2.2 Computing equipment

Reliable and powerful computer systems are required for μ CT analysis to control the scanner; reconstruct the images and to analyse the data. The Skyscan systems are designed to work with standard Microsoft Windows® based computers whereas the Scanco systems are designed to work with 64-bit OpenVMS Unix work stations.

Although image reconstruction using the Feldkamp cone beam algorithm is very computing intensive, it is ideally suited to parallel processing using a cluster of computers. Using a cluster of 4 dual processor workstations and a special cluster version of the Skyscan reconstruction software (NRecon), allows us to reconstruct a dataset in less time than the scan time of a specimen in most cases. Similar cluster software is available for Scanco systems. More recently, versions of the reconstruction software that run on graphics cards (GPUs) have been introduced, and this has lead to a further, substantial reduction in reconstruction times, such that reconstruction is no longer a bottle neck.

The μ CT scanners can produce large amounts of data; at roughly 1GB of data for a 5 μ m scan of a mouse proximal tibia, a Skyscan1172 can easily produce 40-50 GB of data per day, and a Skyscan 1272 system with robotic sample changer easily produces 200GB of data per day. Sufficient data storage and backup capacity is therefore required. We use dedicated file servers with a total storage capacity of

120TB. For data archiving we use a high speed, high capacity tape system (LTO6 Ultrium) that can save approximately 3TB of data per tape. Although high capacity external hard drives are very attractively priced these days, they are in general not very reliable for long term storage.

Analysis of the data is again very computing intensive, and requires the handling of large datasets. Because of the size of the datasets, it is beneficial to use analysis workstations that run a 64-bit operating system such as OpenVMS or 64-bit Windows, as these allow for a larger amount of RAM to be installed. We currently use 64-bit Workstations running Windows 7 that are fitted with 64 or 128GB of RAM and Core i7 processors running at 3.2GHz. Most of the μ CT software is optimised for multi-threading, and therefore the use of systems with as many cores as possible will reduce analysis time.

The whole process of acquiring the X-ray projection images, reconstruction and analysis requires the data to be moved between the file servers and the different types of workstations used. Because of the size of the datasets, this can place severe demands on standard computing networks which are designed to handle relatively small datasets such as text documents and emails. The network can then become a significant bottleneck in the analysis project, and saturation of the network with μ CT data can lead to irritation in colleagues unable to reliably use their computer for their normal daily work. We therefore use a dedicated sub-network (running at 10Gb rather than the more standard 1Gb) connecting the systems used for μ CT, using a dedicated network switch. It is important to select a professional switch with sufficient data-throughput capacity, as many cheap home or office switches struggle to handle the data streams generated by μ CT scanners.

2.3 Other materials

1. Sample holders
2. 4% formalin in phosphate buffered saline
3. Phosphate buffered saline
4. 70% ethanol
5. Parafilm
6. Dremel hobby tool
7. Diamond wafering blade

3. Methods

3.1 *Ex vivo analysis of bone architecture*

There are several scanning parameters to be set up, but the optimal settings will depend on the type and size of the sample, and upon what needs to be analysed.

3.1.1 Sample preparation

Although samples from many species can be analysed using μ CT, the examples here will be based on the analysis of mouse bones. The two most commonly used sites for μ CT analysis of mouse trabecular bone are the proximal tibia and the distal femur since they are easy to dissect out and mount in the scanners. For analyses of cortical bone usually a 1mm section centred in the midshaft is chosen. In many cases the investigator will want to perform histological analysis of samples after scanning. If this is required the bones should be dissected, fixed overnight in 4% buffered formalin, washed in PBS and stored in 70% ethanol prior to scanning. Although μ CT scanning is non-destructive there is a risk of the samples drying out in the scanner due to the heat that is generated. If the specimens will have to undergo mechanical testing

(e.g. bending tests or microindentation) they should be stored fresh frozen before and after scanning. We can wrap the samples in Parafilm® prior to scanning to minimise the risk of this occurring since it has X-ray attenuation similar to water or soft-tissues. Whilst other plastic films can also be used, PVC containing films should be avoided since the chlorine atoms in these can cause attenuation of the X-ray beam. The reconstruction algorithm requires that the sample does not move during the scan, and the samples therefore need to be kept in place using a sample holder. Again care should be taken that the sample holder is relatively transparent to X-rays. We routinely use holders made from 1ml syringes and 5ml pipettes (**Fig. 1a**), drinking straws or polystyrene tubes. These can hold several samples above one another. In combination with the batch scanning options in the Skyscan1172, this means that we can normally load 5-6 samples in a holder and scan these without further user intervention being needed. This will normally take about 1h of scan time, leaving the operator free to do something else. Once the sample has been loaded in the scanner (**Fig. 1b**) and scanner parameters have been set, a scout scan is performed showing the position of the individual samples (**Fig. 1c**). Once the samples' positions have been set and the samples labelled, the scan is started. Using a Skyscan 1272 with robotic sample changer allows the system to scan up to 16 samples without user intervention. When we use this approach, we use 1ml or 2ml syringes with a mark that allows us to position the knee joint at a predetermined position, so that we reliably image the same part of all the samples.

3.1.2 Voltage.

The first parameter to decide on is the X-Ray voltage since this determines the spectrum of X-ray energies. Low voltage shifts the distribution to lower energy X-

rays, while higher voltages shift the spectrum to high energy X-rays. For soft tissue imaging, low voltages around 30-40 kV are generally used whereas for small animal bone samples voltages should typically be set in the 50-60 kV range. Since individual X-ray generators may produce slightly different spectra, even at the same voltage it is best to determine the optimal voltage empirically by trying a small range of voltages with a test sample, and choose the setting that gives the best contrast. We generally use a 60 kV setting for our X-ray source for scanning bone samples using the Skyscan 1272, and 50kV on the 1172 system. Even at this setting the X-ray spectrum contains some low energy rays that negatively affect sample contrast for bone samples but this part of the spectrum can be removed by the insertion of beam hardening filters (e.g. 0.5 mm thick aluminium plate is used on both Bruker and Scanco systems).

3.1.3 Resolution

The next parameter to decide upon is the scan resolution. This depends very much on the nature of the sample and what the researcher is trying to detect. Mouse bone architecture can be imaged very well at a resolution of 4-5 μm (*see Note 1*). This is sufficient resolution to measure the fine trabecular structure, as most mouse trabecular structures have a width in the range of 30-60 μm . As **Fig. 2** shows, reducing the resolution below 10 μm makes it almost impossible to reliably visualise mouse trabeculae. However, rat and human trabeculae are considerably thicker, and 10-20 μm is usually sufficient for rat samples and 20-30 μm for human bone biopsies (**Fig. 2G**). One could of course always scan at the maximum resolution of the scanner, however, this usually leads to much longer scan times and larger datasets that take much longer to reconstruct and analyse. Halving of the voxel size (a voxel is the 3D equivalent of a pixel), for example from 10 μm to 5 μm , leads to an eightfold increase

in file size to image the same volume. Datasets can get so large that standard computers would no longer be able to handle them or take days or weeks to perform the cone-beam reconstruction. It is therefore best to find the best compromise between the minimum resolution acceptable to analyse the details of interest and the scan time. This is paramount especially for *in vivo* applications. **Table 1** shows the effect of scanning resolution on some of the standard measurements for bone. There is relatively little difference between the bone volume of a mouse proximal tibia assessed at 2.5 and 5 μm . The 10 and 20 μm scans however tend to overestimate the amount of trabecular bone. There is also a substantial overestimate of trabecular thickness and trabecular spacing with increasing voxel size, and an underestimate of trabecular number and connectivity. Most of these effects can be explained by the fact that at lower resolutions thinner trabeculae are no longer detected. Also the partial volume effect (when a voxel is part bone and part soft tissue) leads to smearing of the structures, resulting in overestimation of thickness.

The results in **Table 1** show that in most cases a resolution around 5 μm is sufficient for mouse bone, with only a minor benefit of higher resolutions. Although similar trends can be seen when scanning human bone biopsies (**Table 1**), the resolution is much less critical, as the trabeculae and cortical porosities such as Haversian canals in human bone are substantially thicker and scans performed at 10-20 μm are acceptable.

3.1.4 Angle of rotation, rotation step and averaging

A parameter that can be chosen in most scanners is the angle of rotation (180° or 360°). This parameter represents how much the sample should turn during the scan.

While in most applications for quasi-axisymmetric specimens, a rotation of 180° is sufficient, a rotation of 360° is preferable for specimens with more complex shape.

Another parameter to be considered is the rotation step between the individual projection images. A larger step size reduces the number of projection images acquired, and thereby scan time, dataset size and reconstruction time. However, it also negatively affects image quality as **Fig. 3** shows. For a $5\mu\text{m}$ mouse scan a step size in the range of 0.4° - 0.6° usually gives sufficient image quality for bone analysis. An additional step to improve image quality is averaging of several images at each rotation step. This reduces image noise, but can substantially increase scan time.

Averaging also reduces the noise, increases the resolution but increase also the scanning time. In most cases no or small averaging (x2) is sufficient.

On a Skyscan 1172 system a scan of a mouse proximal tibia using our standard settings of 60kV, 0.5 mm Al filter, 180° of rotation, 0.6° rotation step, no averaging, and $5\mu\text{m}$ resolution takes on average 11-12 minutes.

3.1.5 Reconstruction

After the scan has finished, the projection images are loaded into the reconstruction program. This can be done automatically from the control file in Scanco machines or loaded through the NRecon software in Bruker systems. One of the options in the reconstruction steps is compensation for beam hardening. Beam hardening is a μCT artefact resulting from the fact the X-ray tubes used in these systems do not produce X-rays of a single energy, but a spectrum of energies. When the X-rays interact with the sample, those at lowest energies will be absorbed first. The remaining X-rays in the beam will therefore have a higher average energy while passing through the rest of the sample. The result of this is that the outside layer of a sample appears to have

higher X-ray attenuation. Beam hardening correction software tries to correct for this. This can be done in two ways. For Scanco systems the manufacturer provides a correction function (usually polynomial) obtained from scans of beam hardening wedge phantoms with different settings. This equation is then automatically used to correct the grey-levels obtained during the reconstructions step. In Bruker systems, the optimal setting can be assessed empirically for each scanner and type of sample, and for mouse bone samples the values tend to be in the 20-40% range. There are other reconstruction options such as smoothing and ring artefact correction. Although these options will result in images with less noise they can impair the detection of fine details in the image or affect the grey-levels and, therefore, should be used with care for each different application.

Once reconstruction is complete, the dataset can be viewed and analysed.

3.1.6 Calibrations

Sometimes the choice of these scanning and reconstruction parameters is not easy and a lot of work may need to be done to define them for each application. At the end of the day what really counts is the resolution of the image, which is defined as the smallest feature that can be resolved in the image, and is affected by all scanning and reconstruction parameters. One way to test the image resolution for a certain set of parameters is to scan a bar-pattern phantom. These phantoms (for example the microCT and nanoCT bar-pattern phantoms produced by QRM, **Fig. 4**) have a chip with bars with different dimensions and distance between each other. Once scanned and reconstructed, the user can visualise which set of bars can be easily resolved in order to estimate the image resolution. However, it is important to consider that the resolution is also affected by the image artefacts.

It is possible to measure the mineral density of the bone tissue by μ CT. If this is required, a phantom for densitometric calibrations should be scanned and the image reconstructed using the same scanning parameters as the bone samples. Assuming a good linearity of the relationship between the attenuations coefficients and the tissue mineral density in the typical range found for bone tissue (approximately 1200-1400 milligrams of hydroxyapatite per cubic centimetre, mgHA/cc) phantoms with two insertions are sufficient to calibrate the image. Skyscan provides standard mouse (2 mm diameter) and rat (4 mm diameter) HA cylindrical phantoms, each containing a resin loaded with HA at 250 and 750 mg/cm³. Other manufacturers like QRM provide cylindrical phantoms with four or five rods of materials with HA equivalent density up to 1200 mgHA/cc. It should be noted that this density is different from that measured in a DEXA scanner. DEXA scanners measure the average density of a bone, so this is lowered by the contribution of soft tissue. In contrast, the mineral density measured using μ CT represents the mineral content of the mineralised tissue only. It is very important to have optimised the beam hardening correction when measuring density. Averaging of images during image acquisition and small rotation step sizes can also be useful for density measurements as this suppresses noise in the attenuation values, leading to a more accurate measurement. **Fig. 5** shows a slice from a standard mouse femur scan (A) and a scan using 3-frame averaging (B), note the substantial reduction in image noise. When measuring the density, the voxels on the edges of the bone structures should be omitted, as these suffer from the partial voxel effect, resulting in decreased density values. We normally do this by eroding all bone structures by 2 pixels. **Fig. 5C** shows the resulting density distribution from the image in B.

3.1.6 Analysis

A very important facet of the analysis is the selection of a volume, the volume of interest or VOI that can be reproducibly identified in all samples, and contains a reasonable amount of trabecular or cortical bone (*see Note 3*). Mouse bones contain relatively little trabecular bone, and most of this is located close to the growth plates in the proximal tibia and distal femur metaphysis. A good landmark in mouse long-bones is the growth plate. As **Fig. 6** shows, in the mouse tibia and femur the mineralised cartilage can be identified relatively easily, and it forms a bridge across the bone. We select as a reference point the level at which this bridge breaks (**Fig. 6C, D**). For the tibia the volume analysed is then 1mm (200 slices if scans are performed at 5µm) starting 0.1 or 0.2 mm (20 or 40 levels if scans are performed at 5µm) distal to the reference point. A similar method can be used for the distal femur (**Fig. 6A**), but here the volume to be analysed should start 20 or 40 slices proximal from the reference level. Another landmark that can be used is the cartilage of the growth plate. However, the distance of the starting level from the reference level needs to be larger to avoid the primary spongiosa, in the region of 50 slices proximal to the reference level. The next step is separation of trabecular bone from cortical bone. This is usually done manually by drawing in a number of layers (usually around 6-10) distributed through the selected volume (**Fig. 6A**). The software then interpolates to create a separation for the layers in between. However, it is possible to automate the separation of cortical and trabecular bone using image analysis macros, and this substantially reduces hands on analysis time and tends to produce more consistent results.

Next, the bone tissue is separated from the soft tissue using thresholding. The actual threshold value will depend on settings during the scan and the reconstruction stages

(**Fig. 6B and C**). However, finding a good setting is usually fairly straightforward. Once the threshold has been decided on, the same value should be used for all samples within an experiment. Thresholding can often be improved by applying noise reduction filters to the images before the threshold operation. We routinely use a median or Gaussian filter (radius size 1-2) as this very effectively suppresses noise without affecting the edges of structures (**Fig. 6D and E**). Filters based on averaging tend to soften the edges, and this can negatively affect the threshold result. After thresholding has been performed the image can be further cleaned by removing small fragments. As the trabecular bone is a highly connected structure, any unconnected small objects are unlikely to be bone and can therefore be removed using a despeckling operator. The final operator used is the 3D analysis operator; this will perform all the measurement and calculations for the final output data. Table 1 lists the most commonly used parameters. Buxsein et al. (2010) provided a good review of the minimum set of parameters to report in studies where bones are analysed with μ CT (**4**). Bruker and Scanco analyses software packages allow the user to create macros, which will run all the operators in sequence for more efficient analyses.

Although the parameters mentioned above are suitable for analysis of trabecular bone, the cortex is not very well defined at this level. For the analysis of cortical bone, we routinely use a volume of 1mm, starting at a distance of about 3mm from the reference level (**Fig. 4E and F**) or centred at the midshaft if a second scan is performed or the whole tibia is scanned. The thresholding and analysis are then performed as described for trabecular bone. However, one additional operator is usually necessary to deal with pores in the cortex which can negatively influence the average cortical thickness (*see Note 1*). The hole fill operator is run to close these pores before running the analysis operator. Although the main parameter to be studied

are cortical thickness and cortical area, other parameters such as periosteal and endosteal circumference, porosity and shape parameters such as eccentricity, moments of inertia and minimal and maximal bone diameter may also be analysed. Again, for more details about the minimum parameters to report for cortical analyses please refer to the guidelines reported by Bouxsein et al. (2010) (4).

3.2 Analysis of focal bone lesions using μ CT

Analysis of bone architecture in mice requires relatively high-resolution images as described in section **Subheading 3.1**, but there are other applications that do not need such high resolution. One of these is the detection of periarticular erosions, metastases and focal lesions such as occur in models of inflammatory arthritis, cancer and Paget's disease of bone. The lesions are usually large enough to be detected at a resolution of around 15-20 μ m. Detection of bone erosions in the mouse collagen induced arthritis model is fairly straightforward. The arthritis affects hind and rear paws, and the individual paws can easily be imaged in the Skyscan 1172. Scanning should be performed at standard settings of 50kV, 0.5 mm Al filter, 0.6° rotation step but with a 17 μ m resolution. Reconstruction should be performed as described previously, but analysis should be performed slightly differently as the purpose of the scans is visualisation of lesions rather than quantification of the trabecular bone structure. Image filtering and thresholding are performed as described for trabecular bone analysis. However, the final step is not a 3D analysis, but the creation of a 3D model for viewing. Once generated, these models can be freely viewed, rotated, cut outs performed and movies generated using special 3D model viewing software, such as the Skyscan CTVol program. The resulting images clearly show the bone destruction in the arthritic animals compared to the control animals (**Fig. 8A and B**).

We have used a similar technique to detect lytic lesions in a mouse model of Paget's disease of bone (5). One important difference with the arthritis model is however, that the location of the lesions is more difficult to predict. We therefore needed to scan entire mouse legs rather than just a small volume like the proximal tibia. However, even at a low resolution of 17 μ m a single scan can only image part of a mouse leg. The Skyscan1172 allows the researcher to set up “oversize” scans, in which images from several scans can be combined into a single dataset. Once this has been achieved reconstruction and generation of a 3D model should be performed as described for the periarticular erosions mentioned previously. **Fig. 8C and D** show a lytic lesion in a 12-month old transgenic animal. The overview of the femur in **Fig. 8C** was produced by stitching two scans together in software.

3.3 *In vivo* μ CT analysis

The strength of using *in vivo* μ CT scanners is that changes in bone architecture can be monitored over time in individual animals, reducing the inter-subject variability and increasing the ability of measuring early effects of diseases and/or interventions. However, as each scan involves exposure of the animal to radiation, one should ensure that the cumulative dose does not exceed levels that will affect bone metabolism. Also, since the animals need to be anaesthetised during the scan, consideration should be given to the effects of repeated anaesthesia on the animal.

The best area to scan is around the knee since the hind limbs can be easily positioned, and this region is not covered with thick layers of soft tissue. We use a small circular polystyrene holder and masking tape to position and hold the limbs in place (**Fig. 9A**). In fact, when performing *in vivo* scans it is very important to restrain leg movement since this can lead to serious artefacts in the reconstructed images (**Fig. 9C**).

The scanning parameters should be adjusted accordingly. As previously mentioned the smallest voxel size, and consequently the best resolution, obtained with *in vivo* scans is approximately 9-10 μm . An important parameter to optimise in case of *in vivo* scans is the integration time, i.e. duration of each tomographic projection, in milliseconds. Increasing this parameter will on one hand reduce the noise in the image (**Fig. 10**), but on the other hand it will increase the scanning time and therefore the nominal radiation exposure for the animal and the required time of anaesthesia. A compromise should be accepted for each application. In our applications we suggest to use an integration time of 200ms for small (the proximal tibia) or 100ms for large (the whole tibia) regions scanned with a Scanco VivaCT 80. The other parameters should be set up similarly to those described for the *ex vivo* scans. Further details are provided in (6).

Reconstruction and analysis are performed as described for the *ex vivo* scans. However, the limited resolution of the *in vivo* scanners can make thresholding for mouse trabecular bone more difficult. One way to get more reliable threshold results is to use special adaptive thresholding techniques. The wide field of view necessary for scanning of live animals means that the image files at 9 μm resolution are large, and reconstruction times can take several hours per scan, however, by using graphic card accelerated reconstruction this can be reduced to 10-15 minutes..

Moreover, in order to analyse the same region of interest between in the same bone scanned over time or in bones of different animals, a co-registration technique needs to be applied. With this image-processing algorithm two 3D images are virtually overlapped in order to chose the same VOI in the analyses (**Fig. 11**). Both Bruker and Scanco provide rigid registration algorithms that can be run by the provided software packages. Alternatively, external commercial (e.g. Amira, FEI) or

freely available (MeVisLab, Fraunhofer) software packages can be used for this operation. It needs to be considered that every time that an image is rotated the grey-values are interpolated and this may underestimate the density in the border of the bone. Therefore, in some cases it is beneficial to apply the transformation found by the rigid registration operation to the VOI. For more details please refer to (7).

Once the images are overlapped, several analyses can be done to evaluate the spatio-temporal changes of the bone properties. For example changes over time of bone mineral content (BMC) or the bone mineral density (BMD) can be evaluated in different portions of the tibia by using semi-automatic partitioning methods as presented in Lu et al. (8).

4. High resolution imaging

Synchrotron Radiation μ CT (SR μ CT) has significant advantages over standard μ CT thanks to the property of its source, which produces a monochromatic X-Ray beam with high flux and high intensity. These properties allow to reduce the artifacts in the image and to acquire in reasonable time 3D images with high signal-to-noise ratio and resolution. While this technology has huge potential for the characterization of bone features as osteocyte lacunae and canalicular network, unfortunately the access to these facilities is limited due to the requirement of a particle accelerator to produce the high-energy beam. In some cases the scanning speed can be increased by using a polychromatic “pink beam”. As example we report here an image obtained at the Diamond-Manchester Imaging Beamline I13-2 of Diamond Light Source (UK) of a proximal mouse tibia (**Fig. 12**) with the following scanning parameters: 950 μ m C, 2mm Al, 20 μ m Ni filters, ‘pink’ beam (5 to 35 keV), 750 μ m-thick CdWO₄ scintillator with 4x total magnification, effective pixel size of 1.6 μ m, field of view of 4.2x3.5mm,

4001 projection images were collected at equally-spaced angles over 180° and exposure time of 53ms. The total scanning time was approximately four minutes. The projection images were reconstructed using the tomographic reconstruction module of Dawn v1.7. It should be noted that with SR μ CT higher resolution, up to 100-150 nm for fields of view of 100 μ m are possible.

In the last decade high-resolution μ CT scanners have “borrowed” some of the principles of the SR μ CT for improving the achievable resolution in laboratory μ CT systems. Machines that use this approach are manufactured by Zeiss (former Xradia) and achieve resolution of 900 nm (Zeiss Xradia 410 Versa) down to 50 nm (Zeiss Xradia 800 Ultra). Therefore, while similar resolutions can be achieved for small bone specimens as for SR μ CT, with those machines the scanning time is much longer (several hours).

5. Further developments and applications

5.1 in situ mechanical testing

Most μ CT manufacturers also produce kits to perform time-lapse mechanical testing within the μ CT system in order to quantify the deformation of the sample under load. This application has become popular for applications for bone, in particular for trabecular bone specimens tested in compression and vertebral bodies tested in compression and bending in order to investigate the failure mechanism.

Moreover, in the last 15 years image processing algorithms as digital volume correlation (DVC) have been developed to quantify the fields of displacements and strain in heterogeneous bone specimens and biomaterials. This technique allows computing of the 3D field of deformation given two images of a specimen, scanned in an undeformed and in a deformed configuration by finding the map of displacements

that would transform the undeformed image into the deformed one, through an optimization process. Several approaches have been developed, but the description of these is not the aim of this chapter. As an example, a global approach based on the combination of a deformable registration algorithm and a finite element package to post-process the data can be used. While these toolkits provide important quantification of heterogeneous deformation within a bone specimen subjected to loading, we need to stress that before their application particular emphasis should be put in finding the precision of the method for the different scanning parameters, DVC settings, etc. (9).

5.2 Estimation of mechanical properties with finite element models

Furthermore, an exciting development for preclinical applications is the use of computational models to predict the bone mechanical properties from subject specific μ CT images. For example the finite element (FE) method, developed several decades ago for designing mechanical components and complex structures, can be used to predict the bone stiffness and strength for a given μ CT image. This method can be applied both to *ex vivo* and *in vivo* images given a minimal resolution and field of view. Again, the aim of this chapter is not in providing the details of the method, but briefly the standard approach used is (example in **Fig.13**):

- 1) to acquire the bone geometry with the μ CT and reconstruct the image;
- 2) to chose the VOI to be modelled;
- 3) to apply a proper protocol to classify the bony voxels from the background. This is usually done with a similar approach as for the preparation of the images for analyses of bone properties mentioned before, which combines Gaussian or median filter, single level threshold and despeckling;
- 4) to convert all bone voxels into a 8-noded hexahedral finite element;

- 5) to assign homogeneous isotropic material properties to each bony voxel;
- 6) to apply a certain loading scenario ;
- 7) to solve the linear model;
- 8) to post-process the data to estimate the bone stiffness and bone strength.

4. Notes

1. Analysis of cortical porosity in mice may require higher resolution as many pores are smaller than 5 μ m.
2. The NRecon reconstruction software provided by Skyscan requires an additional step. The raw reconstructed image data is in a floating point format, and this is scaled by the software to an 8-bit integer image file. An important step is to choose the correct maximum value from the floating point data and to use the same scaling for all samples in an experiment.
3. For accurate VOI selection bones should be oriented straight. This can be done by positioning the samples correctly in the sample holder. However, due to the irregular shape of bone samples, especially the tibia, it is very difficult to position all samples exactly the same way. The Skyscan Dataviewer allows the user to rotate the image stack along all three major axes, and this can be used to ensure the correct orientation of all samples. This step is extremely important when measuring 2D shape parameters (such as elongation, and minimum and maximum diameter) on single slices of the cortical bone.
4. Buxsein, M.L., Boyd, S.K., Christiansen, B.A., Guldberg, R.E., Jepsen, K.J., Müller, R. (2010) Guidelines for assessment of bone microstructure in rodents using micro-computed tomography. *J Bone Miner Res.* **25**(7), 1468-86.

5. A. Daroszewska, A., Van 't Hof, R., Rose, L., Rose, K., and Ralston, S. (2009) The P392L Mutation of SQSTM1 Causes a Paget's Disease-Like Phenotype In Mice. *J. Bone Miner. Res.* **24 (Suppl 1)**,S38.
6. Oliviero, S., Lu, Y., Viceconti, M., Dall'Ara, E.. (2017) Effect of integration time on morphometric, densitometric and mechanical properties of the mouse tibia. *JBiomech.* **65**
7. Campbell, G.M., Sophocleous, A. (2014) Quantitative analysis of bone and soft tissue by micro-computed tomography: applications to ex vivo and in vivo studies. *BoneKey Rep.* **3**
8. Lu, Y., Boudiffa, M., Dall'Ara, E., Bellantuono, I., Viceconti, M. (2015) Development of a protocol to quantify local bone adaptation over space and time: quantification of reproducibility. *J Biomech.* **49(10)**
9. Dall'Ara, E., Barber, D., Viceconti, M. (2014) About the inevitable compromise between spatial resolution and accuracy of strain measurements for bone tissue: a 3D zero-strain study. *J Biomech.* **47(12)**, 2956-63

Table 1. Influence of scan resolution settings on commonly used μ CT measurements

| Specimen | Resolution | BV/TV | Tb.Th | Tb.Sp | Tb.N | SMI | Conn.Dn |
|--------------|---------------|-------|---------------|---------------|------------------|------|------------------|
| | μm | % | μm | μm | mm^{-1} | | mm^{-3} |
| | | | | | | | |
| Mouse Tibia | 2.5 | 9.05 | 45.40 | 279.89 | 2.15 | 1.91 | 459.69 |
| Mouse Tibia | 5 | 9.17 | 47.94 | 288.79 | 1.91 | 2.10 | 269.88 |
| Mouse Tibia | 10 | 9.75 | 62.27 | 362.93 | 1.57 | 2.27 | 93.26 |
| Mouse Tibia | 20 | 10.64 | 90.66 | 501.52 | 1.17 | 2.51 | 61.31 |
| Mouse Tibia | 30 | 7.55 | 111.41 | 708.19 | 0.68 | 2.67 | 37.41 |
| | | | | | | | |
| Human biopsy | 10 | 15.89 | 159.80 | 736.41 | 0.99 | 1.03 | 5.88 |
| Human biopsy | 20 | 15.43 | 174.44 | 774.31 | 0.88 | 1.14 | 4.66 |
| Human biopsy | 30 | 18.36 | 210.45 | 767.90 | 0.87 | 1.24 | 3.92 |

The proximal tibia from a 3 month old female mouse and a human bone biopsy were scanned at a range of different resolutions and the main trabecular bone measurements performed. BV/TV: percentage trabecular bone volume; Tb.Th: Trabecular thickness; Tb.Sp: Trabecular spacing; Tb.N: Trabecular number; SMI: Structure model index, an indicator whether the trabecular structures are rod-like or plate-like. A lower value indicates a more plate-like structure; Conn.Dn: Connectivity density.

Figures

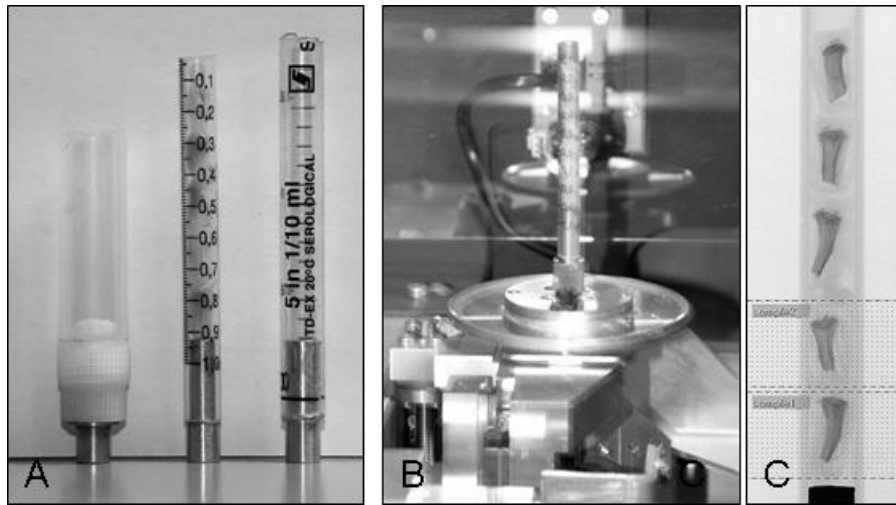


Figure 1: Sample holders and batch scan of multiple samples.

Panel A shows a collection of sample holders made from a centrifuge tube, 1ml syringe and a 5 ml pipette. B shows the sample holder fitted to the sample stage. Panel C shows a scout view of the sample holder with five samples. The bottom two samples have already been set up for scanning.

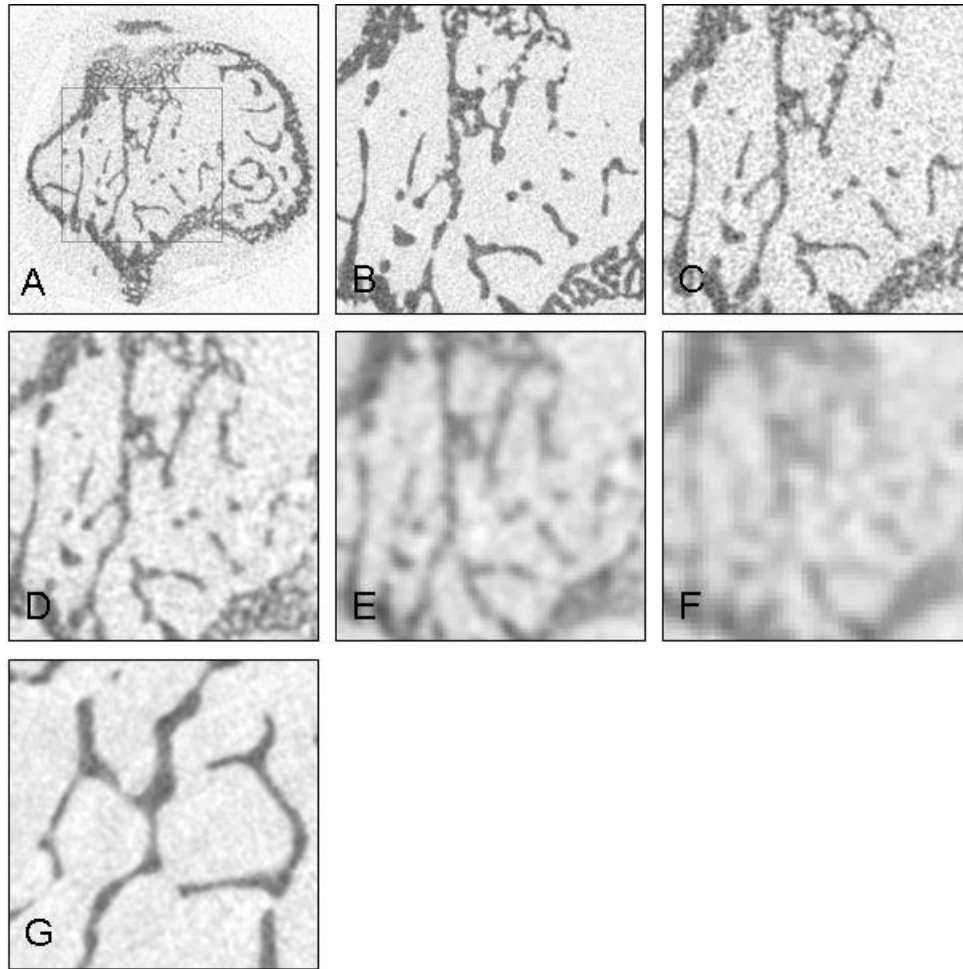


Figure 2: Effect of resolution on image quality.

A mouse proximal tibia was scanned at different resolutions. Panel A shows an overview of a slice and the square indicates the area represented in panels B-F. B: 2.5 μm , C: 5 μm , D: 10 μm , E: 20 μm , F: 30 μm . The image quality of the 5 μm scan in C is good enough for analysis, and even the 10 μm scan (D) provides a reasonable amount of detail. The 20 and 30 μm scans however, are too blurred and lack sufficient detail and contrast for meaningful analysis of trabecular architecture. G: Scan of a human bone biopsy at 30 μm showing sufficient detail for meaningful analysis.

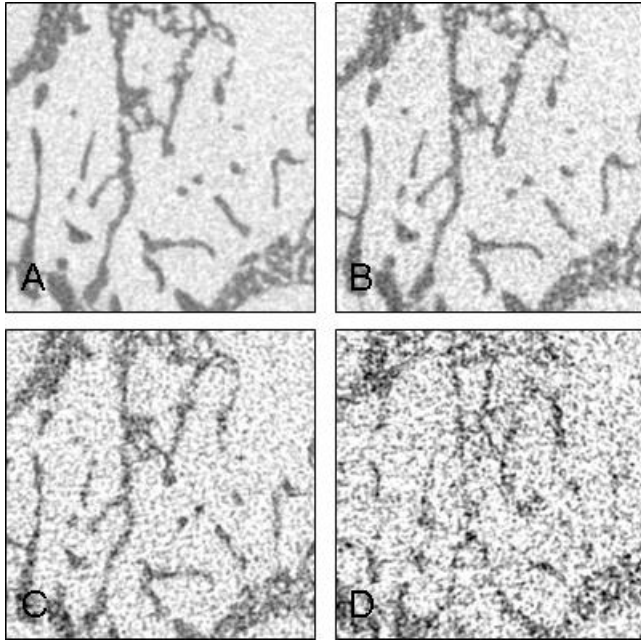


Figure 3: Effect of rotation step on image quality.

A mouse proximal tibia was scanned at 5 μm resolution using different rotation steps. A: 0.2°; B: 0.6°, C: 2°, D: 4°. The image quality increases with decreasing step sizes. Although A shows the best signal to noise ratio, the image acquisition is three times longer and data size three times larger than B, which is still good enough for analysis. The noisy image quality in C and D makes reliable thresholding of the image virtually impossible.

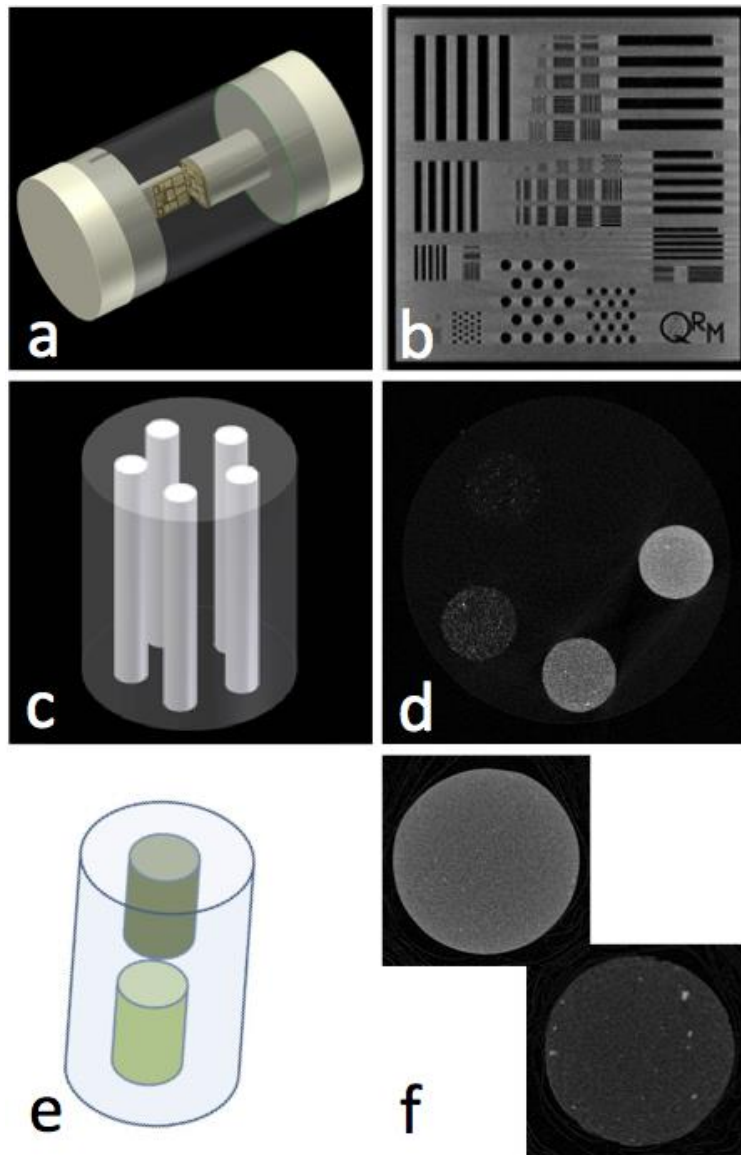


Figure 4: Example of Calibration phantoms.

3D models and reconstructed 2D sections of calibrations phantoms for quality check (QRM microCT bar-pattern phantom reported in *a* and *b*) and for densitometric calibration (QRM phantom with five insertions reported in *c* and *d*; 2-rods Skyscan phantom reported in *e* and *f*).

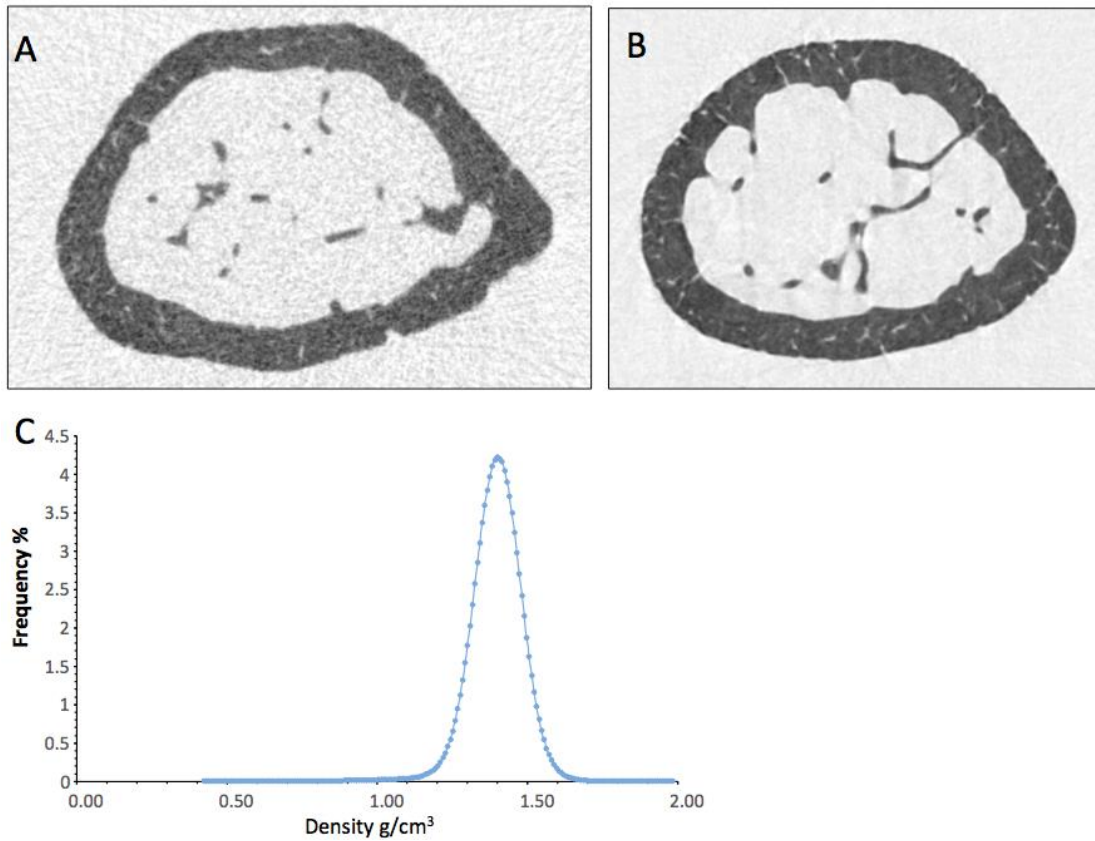


Figure 5: Density measurements after averaging.

A 2D reconstructed slice from a standard mouse femur scan (A) and a scan using 3-frame averaging (B). In C the resulting density distribution from the image in B is reported as frequency plot (histograms).

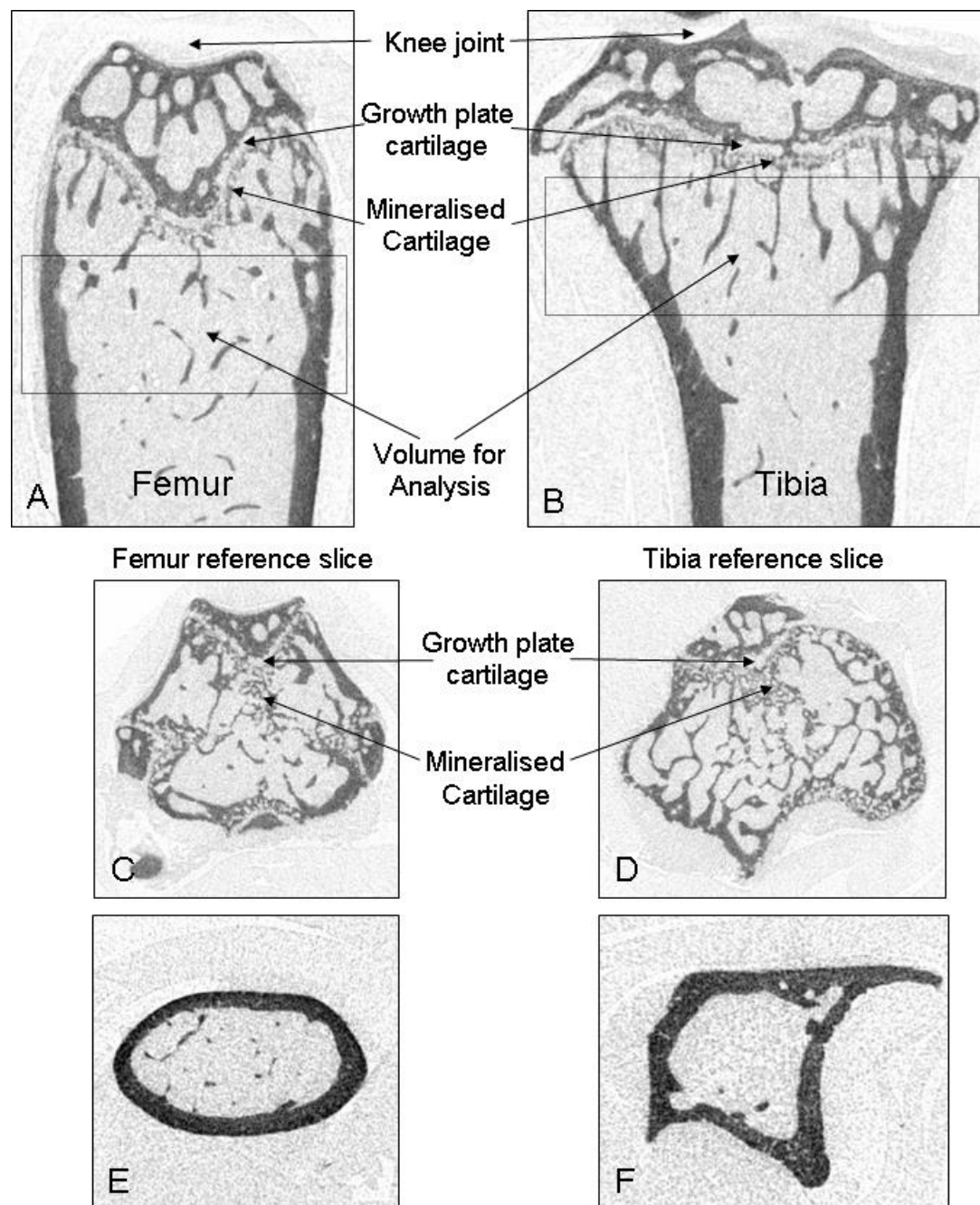


Figure 6: Selecting volumes for analysis.

The boxes in the longitudinal sections of μ CT scans of a mouse femur (A) and tibia (B) indicate the best areas for measuring trabecular bone volume. Landmarks such as the growth plate cartilage and mineralised cartilage are also indicated. C and D: Examples of reference levels where the last bridge of mineralised cartilage has been broken. E and F: slices 600 levels below the reference in the volume used for measuring cortical bone parameters. The shape of the tibia makes measurements from this bone harder to interpret than from the femur.

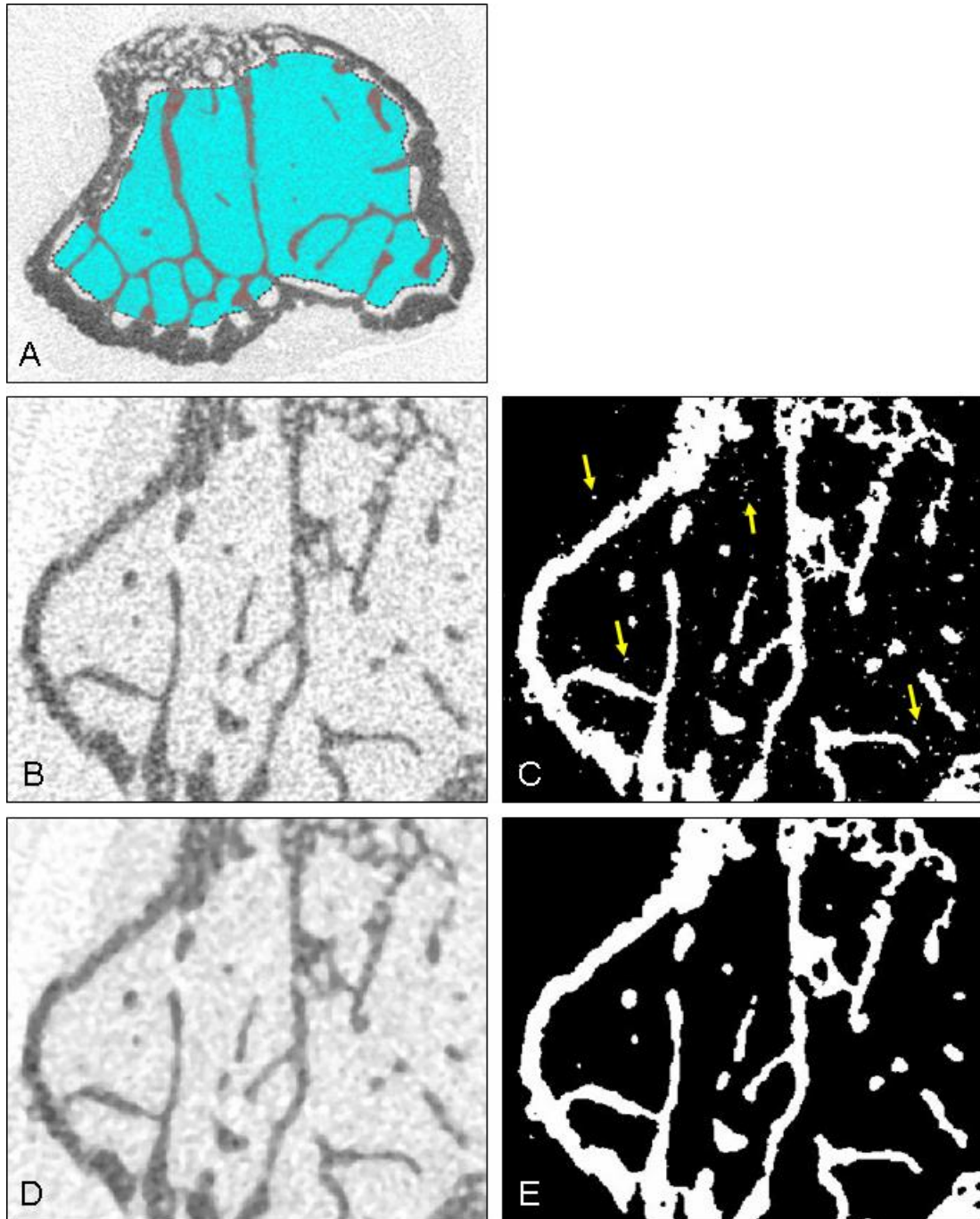


Figure 7: Identifying trabecular bone.

The trabecular bone is manually separated from the cortical bone as indicated by the blue area in panel A. Panel C shows the presence of noise after thresholding the unfiltered image in panel B. Panel E shows the much cleaner effect of the same operation on a median filtered image in panel D. Noise is indicated in panel C by yellow arrows.

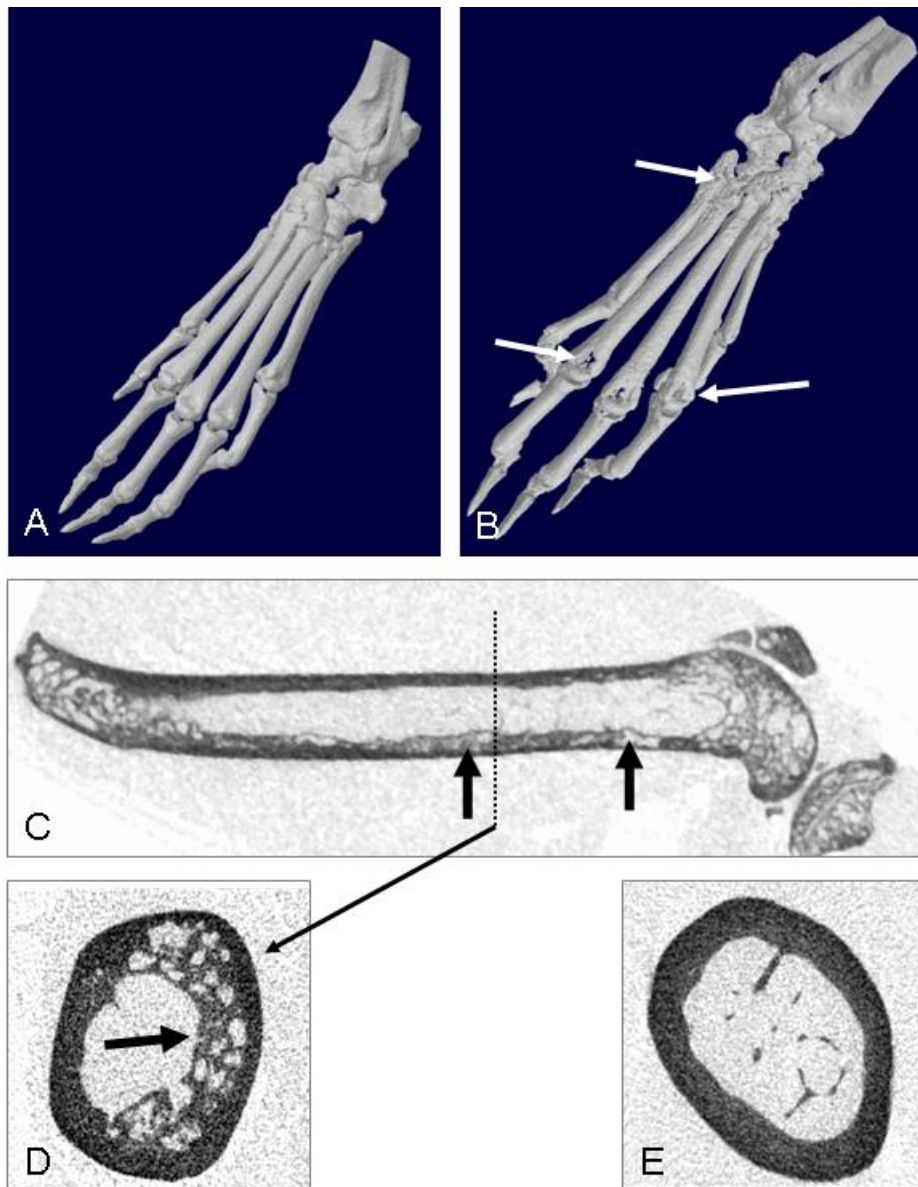


Figure 8: Visualising focal bone lesions

Panel A and B show 3D models of mouse hind paws scanned at 18 μm . A is a control animal, while B is a scan of a mouse 3 weeks after the induction of collagen induced arthritis. Joint destruction is indicated by the arrows in B. Panel C shows a 18 μm scan of the femur of a animal model of Paget's disease. The lytic lesions in the cortex are clearly visible at this resolution. Panel D show a crosssection indicated by the dotted line in C, scanned at 5 μm . Panel E shows the same level from a wild type control mouse. Fig. A and B by E. Coste, R van 't Hof and S.H. Ralston; Panels C-E by A. Daroszewska, R. van 't Hof and S.H. Ralston.

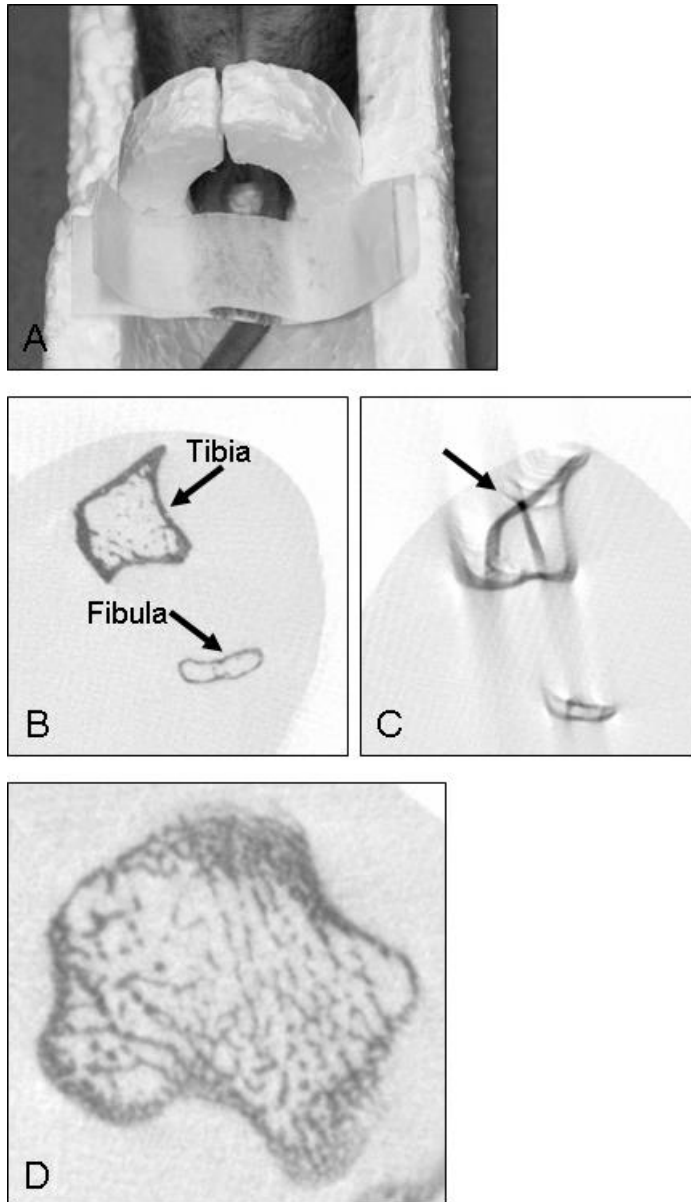


Figure 9: In Vivo scanning.

For proper and reproducible positioning, and to minimise movement, the mouse legs are inserted into a polystyrene ring and the feet taped together (A). Panel B shows a slice from a good 9 μm scan of the tibia and fibula of a 4 month old mouse. Panel C shows the artefacts resulting from leg movement during the scan. Panel D shows the amount of trabecular detail that can be obtained from in vivo scans of mouse bone.

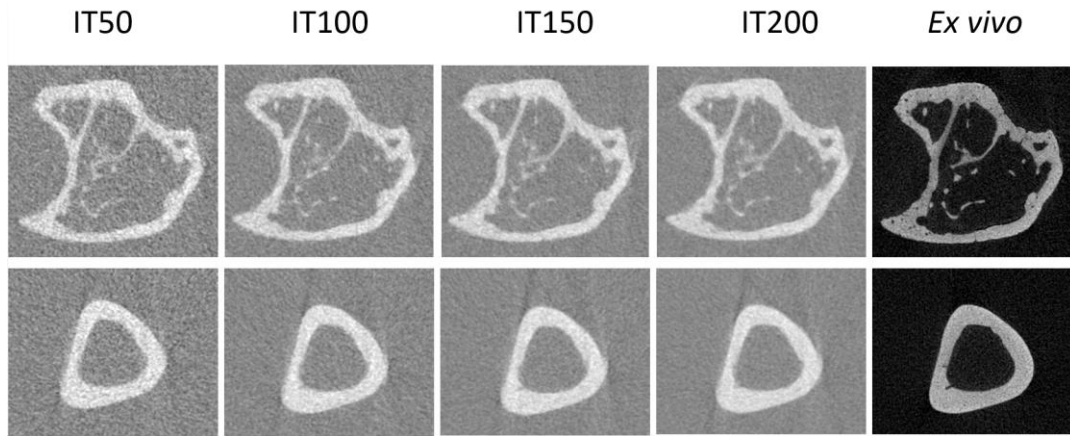


Figure 10: Effect of integration time in *in vivo* scans.

In *in vivo* imaging the integration time is an important parameter to set for finding the best compromise between the scanning time (and therefore the radiation dose and the time with the animal under anaesthesia) and the image quality (and therefore the measurement uncertainties). In this figure we report two cross-sections (top: proximal part including trabecular and cortical bone; bottom: tibia midshaft) of a mouse tibia scanned with four sets of *in vivo* scanning parameters (Scanco VivaCT80: from left to right with integration time equal to 50, 100, 150 and 200 ms, respectively; all the other parameters were the same: voxel size 10.4 μm , 55 kV, 750 projections/180°, 0.5 mm Al filter) and a set of *ex vivo* scanning parameters as gold standard (Skyscan1172: 4.35 μm voxel size, 50 kV, current: 179 μA , exposure time: 1180 ms, 180° rotation, 0.7° rotation step, 0.5 mm Al filter). *Note: for this figure the grey-scale images were inverted in order to underline the noise in the bone tissue.*

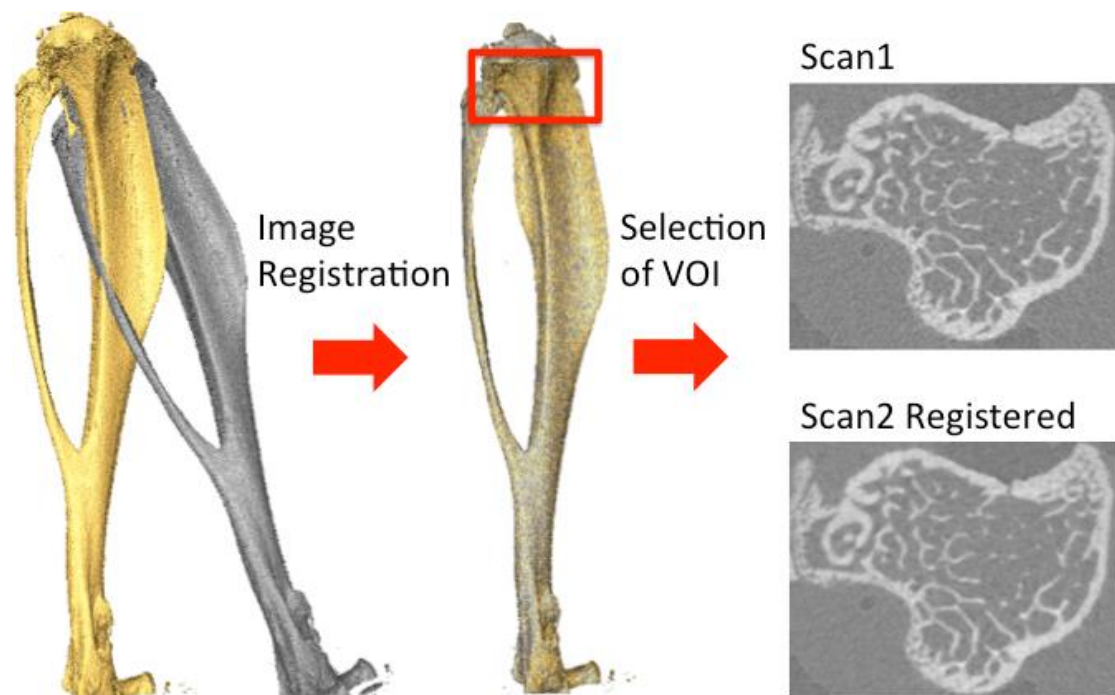


Figure 11: Image registration.

The rigid image registration algorithm can be used to overlap the images of the same bone scanned in vivo at two different time points (in the example Scan1 and Scan2) in order to choose the same volume of interest (VOI) to be analysed.

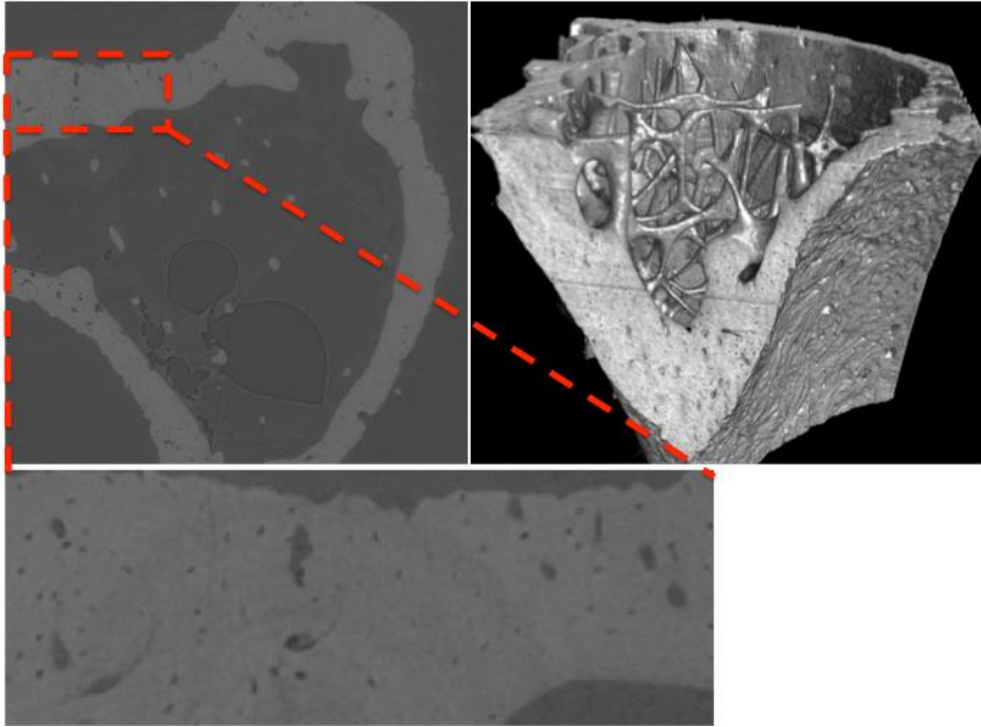


Figure 12: Image obtained with Synchrotron μ CT.

Example of image obtained with SR μ CT for a proximal mouse tibia acquired with voxel size of 1.6 μm . Even for large fields of view this image modality allows to perform high-resolution scans in short time (approximately four minutes in this case). The resolution can be increase up to 100 nm if the field of view is reduced to approximately 100 μm .

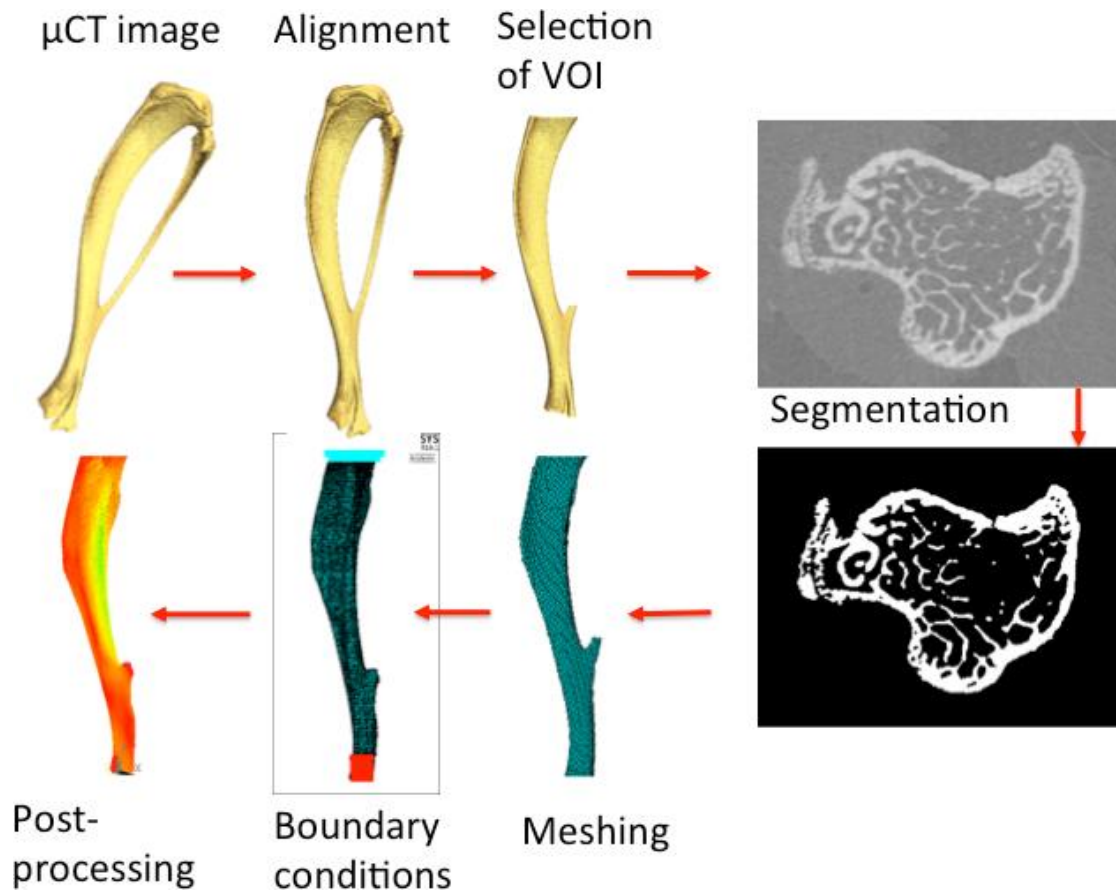


Figure 13: Procedure to convert a μ CT image into a finite element model.

Example of the procedure to generate a FE model from a μ CT after it has been reconstructed. From the model different parameters can be extracted, as the bone stiffness, the bone strength as well as the distributions of displacements, strains and stresses.